



Green synthesis and characterization of hydroxyapatite bio composite using *Azadirachta indica* A. Juss. bark extract and *in-vitro* biocompatibility with human osteoblasts cells

Venkatachalam Murugesan, Manju Vaiyapuri

Department of Biochemistry, School of Bioscience, Periyar University, Salem, Tamil Nadu, India

Abstract

Hydroxyapatite (HA) is good biocompatibility and bioactivity it's excellent candidate for bone repair and substitution due to Ca/P ratio similar to natural bone. The the present study is synthesis HA by a wet chemical method using synthetic precursor composite with neem plant (*Azadirachta indica*) bark extract (AI) and to evaluate the antibacterial activity. Synthesised HA was characterised by using X-ray diffraction (XRD), Fourier transforms infrared spectroscopy (FT-IR) and Scanning electron microscope (SEM). The conformation of HA biocomposite was fabricated to polycrystalline hydroxyapatite exhibit hexagonal crystal structure. In addition to that, HA composite to analysis gram positive and gram negative bacteria such as *Escherichia coli*, *Bacillus subtilis*, and *Staphylococcus aureus* was evaluated by agar and disc diffusion method. Cytotoxicity activity was measured by using cell proliferation activity was observed on osteoblast MG-63 cell line. This study suggested that - synthesized biocomposite of HA with neem bark extract an effective substitute for synthetic starting material to bone tissue engineering.

Keywords: *Azadirachta indica*, Bark, hydroxyapatite, antibacterial, cell viability

Introduction

The bio ceramics are excellent bio-active material and widely used for bone tissue engineering. The mineral phase (CaP) of the hydroxyapatite is itself mimic the natural bone [1]. It may also biomaterial is natural or synthetic that comprises whole/part of a living things which is performs, augments and replaces a natural function. Consequently a biomaterial is important material that is used as implant for orthopaedic application, versatile application in heart valve and it used as bioactive and bone and hip replacement. Similarly the bone and joint gradually deteriorates affect millions of people across the world. The ultimate aims of the regeneration of damaged tissues with restoring and maintaining the function of vertebrate animal bone tissues using the combination of cellular biology with metal composite materials [2].

Hydroxyapatite ($\text{Ca}_{10}(\text{PO}_4)_6(\text{OH})_2$) has been broadly used in the orthopaedic and dental application and it's biocompatibility, bioactive and osteo conductivity [3-5]. The substantial elemental and biological properties of hydroxyapatite are showed to be restricted by its crystal structure and composition. Consequently the modern researcher to develop such as HA coated materials [6,7]. One of the major issue in orthopaedics is a bone infection caused by the pathogenic organism [8]. Hence, modern researcher hydroxyapatite were combination with antibiotics is useful for the preparation of biomaterial filling bone defects [9].

In previous research report described about the hydroxyapatite substitute with the silver ions to resolve this bacterial infection case [10]. To addition that the green synthesis of nanoparticles from plant derived has started a new era to deal in pathogenicity assay [11]. However, the green synthesis of nanoparticles to composite to bone regeneration is still need to exploration. The present study was attempt to green synthesis of hydroxyapatite substitute and antibacterial properties with bone regeneration assays.

Azadirachta indica each part of has been used for anmedication from ancient times [12,13]. *Azadirachta indica* bark used in the traditional system of medicine [14]. Neem bark contain antiseptic, antibacterial and anti-tumour activities [15]. To the best of our knowledge, there is few reports in the scientific literature on the HA nanorods using neem extracts. Hence, the current study is aimed to synthesize HA using neem bark extract.

Materials and Methods

Azadirachta indica bark extract

Azadirachta indica bark was collected from Periyar University Campus Salem, India. The voucher was authenticated in the Department of Botany, Periyar University and safeguarded. The bark was detached and washed twice with running tap water followed by double distilled water. The neem bark was placed in dark shade condition until proper drying. The dried bark grind with mortar and pestle to make them as a powder. Five gram of neem bark powder was dissolved in fifty millilitres (50mL) of double distilled water, and then heated for 30 minutes, and cooled down followed by filtered using whatman No.1 filter paper. The filtered extracted was kept at 4 °C for further use.

Synthesis of HA-AI

Hydroxyapatite synthesis using neem bark extract by wet chemical method [16] with minor modification. Calcium nitrate and di-ammonium hydrogen phosphate were used as the precursors. One molar (1M) of calcium nitrate ($\text{Ca}(\text{NO}_3)_2 \cdot 4\text{H}_2\text{O}$) and diammonium hydrogen phosphate ($(\text{NH}_4)_2\text{HPO}_4$) – (0.6 M) was prepared in double distilled water. The ratio of Ca/P was maintained with di-ammonium hydrogen phosphate solutions were titrated to be added dropwise into calcium nitrate solution under vigorous stirring at room temperature for 20 minutes, solution were adjusted to pH10

was using for (0.8M) Sodium hydroxide (NaOH) to attain their purity. Finally the solution appeared in pale white colour precipitate. The reaction mixture was then stirred for 1 h and kept at room temperature for 24 h. The obtained precipitate was spin (4500rpm) to separate by product and then dried at 150 °C for 6h in hot air oven (Labline, India). Finally, the dried cakes were crushed into obtain powder. Further the sample to check their nature to investigate their activity.

Fourier Transform Infrared Spectroscopy

The Fourier transforms infrared spectra (FT-IR) was performed to identify the functional group of the hydroxyapatite with *A. indica* (HA/AI). The spectrum was recorded using (FTIR, Bruker Tensor 27) by KBr Pellet method. The representative of the sample was mixed with 100 mg KBr pellet and also pressed into discs analysed in different wave number range 400-4000 cm^{-1} at a resolution of 4 cm^{-1} in FTIR spectroscopy.

X-ray diffraction analysis (XRD)

The structure and crystalline phase of the HA/AI were studied by using X-ray diffraction patterns, in the model of a RigakuMiniflex-II diffractometer. Powder XRD taken in range between 20°-60° using Cu Ka monochromatic radiation (1.5406 Å). The crystallographic identification of the sample was accomplished by correlate the experimental XRD pattern with JCPDS data.

Scanning Electron Microscopy (FESEM) analysis

The morphology of the synthesized HA/AI was observed using a scanning electron microscope (SEM).

Antibacterial activity of HA/AI

Antibacterial activity of HA/AI was evaluated by both agar well and disc diffusion method against clinical pathogens *Escherichia coli* (MTCC 443 - Gram negative bacteria), *Staphylococcus aureus* (MTCC 6671 - Gram-positive bacteria), *Bacillus subtilis* (MTCC441 - Gram-positive bacteria) [17]. The pure cultures of bacteria were swabbed uniformly on the individual plates using sterile cotton swabs on the Mueller Hinton agar. Five wells were made on 7 mm in diameter in Muller Hinton agar plates by using corn borer. The inoculation of the three different pathogens broth culture were prepared and incubated at 37°C for overnight. HA/AI was loaded into different concentrations (60, 80, 100, 120 mg/ml). The plates were kept for 24 hrs at 37°C. The microbial zone of inhibition was measured after the inhibition period and tabulated. Furthermore the images were documented. Same culture methods were followed for swabbing process and the different concentration of HA/AI was loaded in a sterile disk plate to determine for the disk diffusion method.

MTT assay

To determine the cell viability, we used the tetrazolium dye (MTT, Sigma Aldrich) by the method of Balashanmugam *et al.* [18]. In brief, the MG-63 cells were seeded in 96-well plates (4×10^3 cells/well), cultured and allowed to adhere overnight. Following incubation period for 24 hr, the cells acquired typical confluences; the supernatant medium was replenished using different concentrations of hydroxyapatite in complete medium and DMSO for 24 hr. At the end of each treatment, DMSO medium in the well was removed

and add 50 μl MTT reagent (conc. 0.5 mg/mL). Then, the wells were kept in a dark condition for 4 hr at 37°C. Medium with MTT was discarded and 200 μL DMSO added to solubilize the formazan blue (3-[4, 5-dimethylthiazol-3-yl]-2, 5-diphenyl tetrazolium Bromide) crystals. The percentage viability was measured at 570 nm using an ELISA plate reader.

Statistical analysis

The research data was conducted in (n=3) in triplicates. Results were expressed in means \pm standard deviation (SD).

Result and Discussion

Fourier Transform Infrared Spectrometer analysis

Hydroxyapatite (HA) with *A. indica* bark (AI) extract was successfully synthesized (HA/AI) by green synthesis methods. The green synthesised method is more advantages and suitable for them could be ability to reduce the crystal size (morphology) and a cost of effective. HA/AI is high purity and environmental non-toxicity so they are most efficient method [16]. FTIR spectrum is obtained of the product is showed in the figure 1. The characteristic PO_4^{3-} vibrations of HA/AI is appeared at 558 and 600 cm^{-1} , along with other phosphate peaks at the 474, 1023, 1069 and also 1076 cm^{-1} respectively. If the bands are 3543 characteristic O-H stretching peaks are respectively. The broadband are extending from the 2002 to 3405 cm^{-1} is attributed to the stretching modes of the water molecules (H_2O). The positions of these peaks clearly indicate to the formation of B-type carbonated hydroxyapatite and A-type carbonated hydroxyapatite.

FTIR spectra of the as synthesized samples showed that hydroxyapatite with *A. indica* is different vibration mode was intensified similar to synthetic hydroxyapatite [8]. The account of HA/AI biomaterials is often depends on functional group and their features. The present study reported *A. indica* bark with hydroxyapatite has a functional group to provide network arrangement is good biocompatibility.

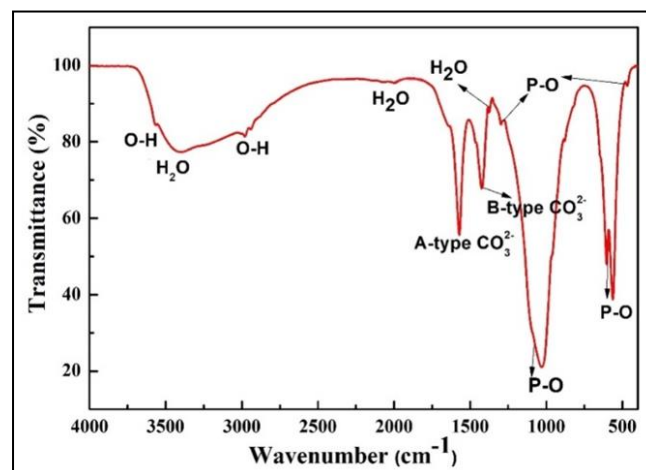


Fig 1: FTIR Pattern of HA/AI from *A. indica* bark.

XRD analysis

Figure 2 showed that x-ray diffraction pattern (XRD) pattern of the synthetic composite is good agreement with the JCPDS cards for hydroxyapatite (JCPDS file No. 09-0432) with the hexagonal crystal structure using the standard Debye-Scherrer approaches. The broad peaks in

ranges between 20° – 80° can be described to (211), (112), (300) and also (202) reflection of hydroxyapatite (HA/AI) to get overlapped the resulting in different broad peak which suggests that the existence of less crystalline and also nano-sized particles. The average crystalline size of the sample was found to be 53.8nm.

Powder XRD characterization pattern represented the (HA/AI) crystal phase and crystal structure mainly in Ca/P network in JCPDS standard data to lattice in amorphous nature. The correlation between pure hydroxyapatite and composite AIB/HAs groups phase purity^[3,9].

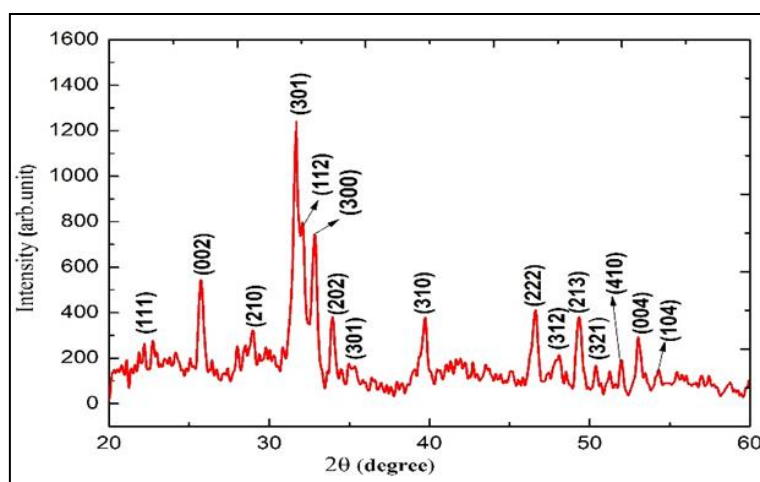


Fig 2: XRD pattern of HA/AI from *A. indica* bark.

SEM

Micro-structural observation by SEM and EDAX is revealed synthesized HA/AI composite is shown in Fig. 3 (a-b). The composite material was exhibited in non-uniform agglomerates of elongated particles like flower like shape which can be seen in figure. From the HA/AI formation by the elongated discrete particles with spherical like structure. This micro particles were found to be homogeneously distributed with aggregation. The EDAX spectrum of bio-composite which is showed the presence of elements Ca, P, O and C respectively. From the SEM morphology, it can be clear that the HA/AI bio-composite^[6] provide most favourable morphology for nano-structured drug designing.

Antibacterial activity

The hydroxyapatite (HA/AI) was evaluate against antibacterial activity using on *Escherichia coli*, *Staphylococcus aureus* and *Bacillus subtilis* were evaluated by agar well diffusion method and also disc diffusion method. Figure 4 is showed antibacterial activity the zone of inhibition was recorded in Table 1. The composite material of HA/AI showed moderate zone of inhibition was observed on *E.coli*, *S. aureus* and *B. subtilis*. Whereas in the case of *E. coli* and *S. aureus* begins at 100 μ l and 120 μ l the activity was increased when increasing concentration of HA/AI. The *S. aureus* growth was more inhibited (5mm) at 60 μ g/ml of HA/AI followed by *B. Subtilis*. The minimal inhibitory activity of HA/AI against *S. aureus* was found.

Table 1: Antibacterial activity of HA/AI from *A. indica* bark

| Pathogens | Concentration (mg/ml) | | | |
|--|-----------------------|----|-----|-----|
| | 60 | 80 | 100 | 120 |
| <i>Escherichia coli</i> | - | - | 9 | 18 |
| <i>Staphylococcus aureus</i> | 5 | 7 | 8 | 7 |
| <i>Bacillus subtilis</i> (Disc method) | 2 | 4 | 8 | 6 |

Table 2: Cell viability of HA/AI from *A. indica* bark

| Concentration (μ g/ml) | Percentage of cell growth (%) | | |
|-----------------------------|-------------------------------|----------|----------|
| | 12 hours | 24 hours | 48 hours |
| 10 | 16.14 | 16.47 | 28.00 |
| 20 | 19.76 | 26.35 | 31.30 |
| 30 | 29.65 | 34.59 | 39.53 |
| 40 | 36.24 | 42.83 | 44.48 |
| 50 | 46.12 | 52.71 | 54.36 |
| 60 | 52.71 | 59.30 | 64.25 |
| 70 | 62.60 | 67.54 | 75.78 |
| 80 | 69.19 | 72.48 | 80.72 |
| 90 | 79.07 | 84.01 | 85.66 |
| 100 | 82.37 | 90.60 | 96 |
| IC ₅₀ | 56.91 | 47.42 | 45.98 |

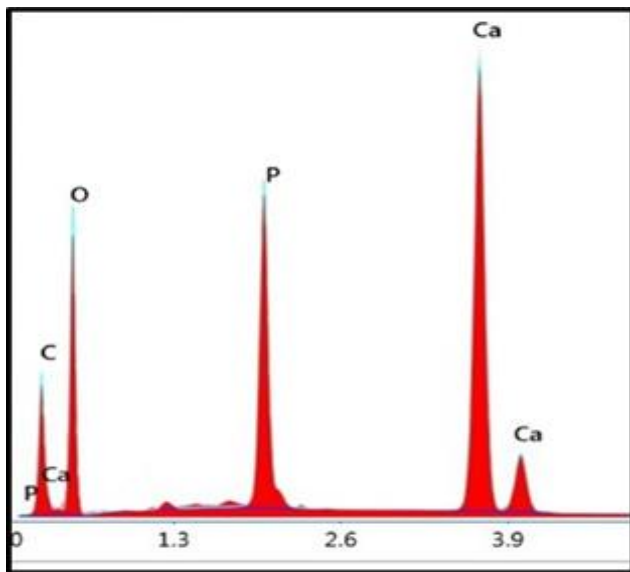
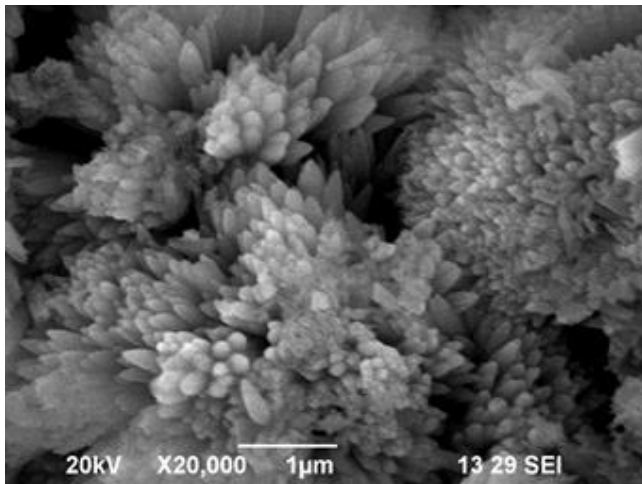


Fig 3: SEM and EDAX of HA/AI from *A. indica* bark.

Antibacterial activity of the composite of HA/AI is involved in two major processes, protein downregulation and interrupt (destroyed) the bacterial membrane (Glycan) connections between (compartments) them [19]. In fact that

bacterial growth could be considerably inhibited in a dose dependent manner. From the previous report showed that bacterial effect against Gram-negative bacterium *E. coli*, it is slightly higher than colloidal silver nanoparticles systems [20].

MTT assay

Cell cytotoxicity is most fundamental issues for nanomaterials are good biocompatibility for bone implant field. Figure 5 showed HA/AI composite material cell viability was examined under the osteoblast, MG-63 cell line. The MG-6 cells morphological changes were observed by using different dose manner (10-100µg/ml). The MTT assay was performed by different concentrations with three different incubation periods 12 hrs, 24 hrs, 48 hrs respectively. The samples were providing at 10 µg/ml, of cell ability range 16.14 % at 12 hrs. Interestingly, increasing the concentration of HP/AI (20 to 50 µg/ml) cell viability slightly increased according to corresponds value, 31.30%, 39.30%, 44.48%, and 54.36% respectively. It is noted that the MG-63 cell growth was increased as dose dependent manner consequently the composite sample didn't interrupt the cells morphology. The cell mortality rate compared to three different intervals period will be HA/AI. Growth rate of MG-63 cells with HA/AI for excellent biocompatibility candidate to composite materials. MTT assay are clearly proved, due to the HA/AI biomaterial is non toxicity (Figure 6). The clearly observed the synthetic hydroxyapatite with HA/AI composite does not interrupt the normal cell growing and cell toxicity. This may be due to the fact that neem does not affect the human cells MG-63. Despite fact that, it could promote cell growth and potent will be anti-cancerous and apoptotic activities. It is also close agreement with excited data on the synthesis and characterization of coated hydroxyapatite different phase layer [21]. According to our present study, the neem bark composite HA/AI indicating their biocompatibility and suggesting that their suitable for good candidate would be beneficial as implants for bone regeneration. Clinical trials are needed to prove these claims and also novelty.

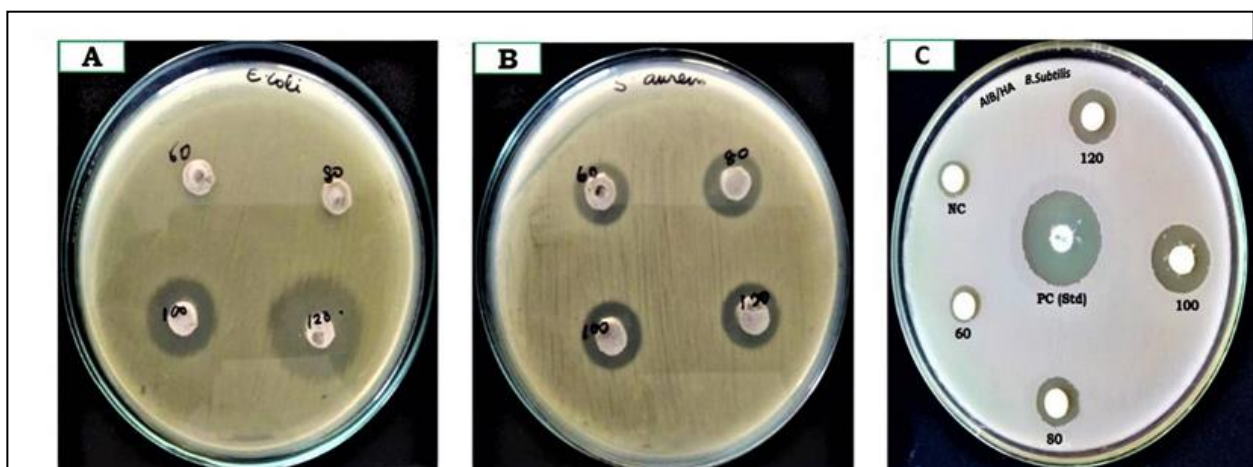


Fig 4: Photograph of the antibacterial activity of of HA/AI from *A. indica* bark against clinical pathogens a) *Escherichia coli* b) *Staphylococcus aureus* c) *Bacillus subtilis*

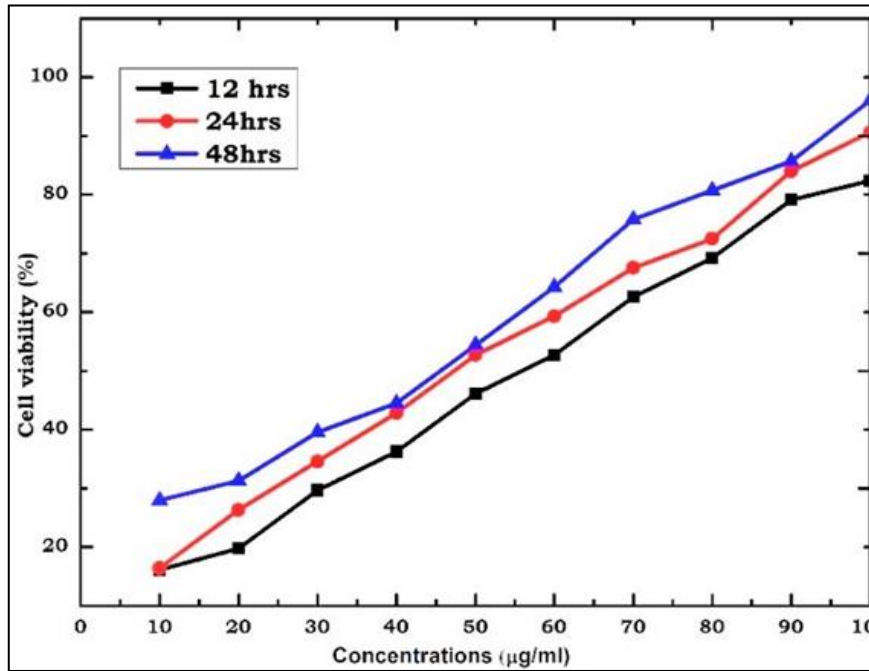


Fig 5: Cytotoxicity of MG-63 cells treated with 10-100 µg/ml of the HA/AI from *A. indica* bark after 12, 24 and 48 hrs.

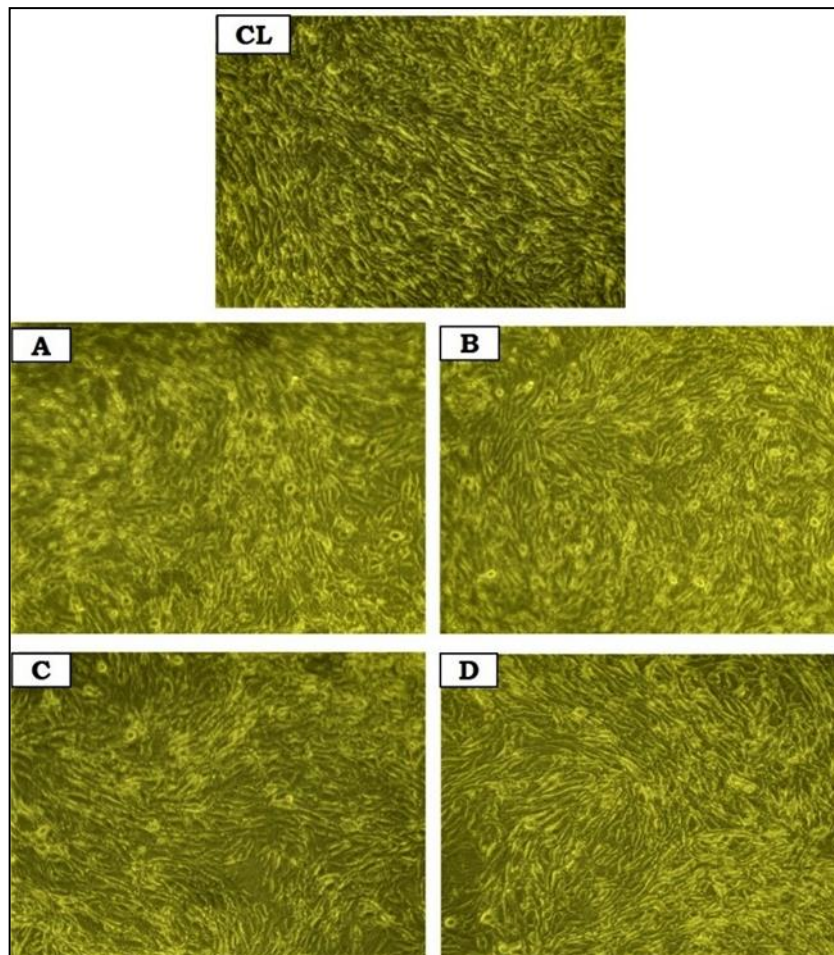


Fig 6: Morphological of human osteoblast (MG-63) with different concentration of HA/AI from *A. indica* bark. Here, CL-Control, (a) 25µg/ml (b) 50µg/ml (c) 75µg/ml (d) 100µg/ml.

Conclusion

The present study report conclude as-synthesized hydroxyapatite which are efficiently incorporated in green synthesis of HA/AI composite materials. The FTIR and XRD spectral analysis conclude that all functional group

corresponding to composite hydroxyapatite material. Furthermore the value correlate with JCPDS standard data to lattice in amorphous nature. Similarly the SEM-EDAX image of sample exhibited to the better morphology. Furthermore the plant bark based hydroxyapatite excellent

antibacterial activity against clinical pathogens. Finally, the cell viability was proved as-synthesized composite does not interrupt the normal cell growing MG-63 cells. The *in vitro* cytotoxicity studies indicate these composite materials are non-toxic. Hence, the green synthesis of HA/AI composite could be a potential candidate in osteology field.

Conflict of interests

The authors declare no conflict of interest.

Reference

- Kim T, See CW, Li X, Zhu D. Orthopedic implants and devices for bone fractures and defects: Past, present and perspective. *Eng Regen*,2020,1:6-18. doi:10.1016/j.engreg.2020.05.003
- Ustriyana P, Schulte F, Gombedza F, ur na, 2021.
- Muthu D, Gowri M, Suresh Kumar G, Kattimani VS, Girija EK. Repurposing of antidepressant drug sertraline for antimicrobial activity against *Staphylococcus aureus*: a potential approach for the treatment of osteomyelitis. *New J Chem*,2019,43(14):5315-5324. doi:10.1039/C8NJ06297H
- Kumar GS, Girija EK. Flower-like hydroxyapatite nanostructure obtained from eggshell: A candidate for biomedical applications. *Ceram Int*,2013,39(7):8293-8299. doi:10.1016/j.ceramint.2013.03.099
- Laranjeira MS, Moço A, Ferreira J. Different hydroxyapatite magnetic nanoparticles for medical imaging: Its effects on hemostatic, hemolytic activity and cellular cytotoxicity. *Colloids Surfaces B Biointerfaces*,2016,146:363-374. doi:10.1016/j.colsurfb.2016.06.042
- Chozhanathmisra M, Murugan N, Karthikeyan P, Sathishkumar S, Anbarasu G, Rajavel R, *et al.* Development of antibacterial activity and corrosion resistance properties of electrodeposition of mineralized hydroxyapatite coated on titanium alloy for biomedical applications. *Mater Today Proc*,2017,4(13):12393-12400. doi:10.1016/j.matpr.2017.10.009
- Sergi R, Cannillo V, Boccaccini AR, Liverani L. Incorporation of bioactive glasses containing Mg, Sr, and Zn in electrospun PCL fibers by using benign solvents. *Appl Sci*, 2020, 10(16). doi:10.3390/app10165530
- Kumar GS, Rajendran S, Karthi S. Green synthesis and antibacterial activity of hydroxyapatite nanorods for orthopedic applications. *MRS Commun*,2017,7(2):183-188. doi:10.1557/mrc.2017.18
- Nagaraj A, Samiappan S. Presentation of Antibacterial and Therapeutic Anti-inflammatory Potentials to Hydroxyapatite via Biomimetic with *Azadirachta indica*: An *in vitro* Anti-inflammatory Assessment in Contradiction of LPS-Induced Stress in RAW 264.7 Cells. *Front Microbiol*,2019,10. doi:10.3389/fmicb.2019.01757
- Micsonai A, Wien F, Kernya L. Accurate secondary structure prediction and fold recognition for circular dichroism spectroscopy. *Proc Natl Acad Sci U S A*,2015,112(24),3095-3103. doi:10.1073/pnas.1500851112
- Rathi Sre PR, Reka M, Poovazhagi R, Arul Kumar M, Murugesan K. Antibacterial and cytotoxic effect of biologically synthesized silver nanoparticles using aqueous root extract of *Erythrina indica* lam. *Spectrochim Acta - Part A Mol Biomol Spectrosc*,2015,135,1137-1144. doi:10.1016/j.saa.2014.08.019
- Gupta SC, Prasad S, Tyagi AK, Kunnumakkara AB, Aggarwal BB. Neem (*Azadirachta indica*): An Indian traditional panacea with modern molecular basis. *Phytomedicine*,2017,34,14-20. doi:10.1016/j.phymed.2017.07.001
- Subapriya R, Nagini S. Medicinal properties of neem leaves: A review. *Curr Med Chem - Anti-Cancer Agents*,2005,5(2),149-156. doi:10.2174/1568011053174828
- Pandey MM, Rastogi S, Rawat AKS. Indian traditional ayurvedic system of medicine and nutritional supplementation. Evidence-based Complement Altern Med, 2013. doi:10.1155/2013/376327
- Biswas K, Chattopadhyay I, Banerjee RK, Bandyopadhyay U. Biological activities and medicinal properties of neem (*Azadirachta indica*). *Curr Sci*,2002,82(11),1336-1345.
- Dadashpour M, Firouzi-Amandi A, Pourhassan-Moghaddam M. Biomimetic synthesis of silver nanoparticles using *Matricaria chamomilla* extract and their potential anticancer activity against human lung cancer cells. *Mater Sci Eng C*,2018,92,902-912. doi:10.1016/j.msec.2018.07.053
- Santhosh S, Manivannan N, Ragavendran C. Growth optimization, free radical scavenging and antibacterial potential of *Chlorella* sp. SRD3 extracts against clinical isolates. *J Appl Microbiol*,2019,127(2),481-494. doi:10.1111/jam.14336
- Balashanmugam P, Durai P, Balakumaran MD, Kalaichelvan PT. Phytosynthesized gold nanoparticles from *C. roxburghii* DC. Leaf and their toxic effects on normal and cancer cell lines. *J Photochem Photobiol B Biol*,2016,165,163-173. doi:10.1016/j.jphotobiol.2016.10.013
- He F, Yang Y, Yang G, Yu L. Studies on antibacterial activity and antibacterial mechanism of a novel polysaccharide from *Streptomyces virginia* H03. *Food Control*,2010,21(9),1257-1262. doi:10.1016/j.foodcont.2010.02.013
- Ansari S, Khorshidi A, Shariati S. Chemoselective reduction of nitro and nitrile compounds using an Fe₃O₄-MWCNTs@PEI-Ag nanocomposite as a reusable catalyst. *RSC Adv*,2020,10(6),3554-3565. doi:10.1039/c9ra09561f
- Chen R, Shen J *Journal Pre-proofs*. 2019.